Simultaneously Emerging Braitenberg Codes and Semantic Compositionality

Yuuya Sugita
Department of Psychology III (Cognitive Psychology)
University of Würzburg
Röntgenring 11, 97070 Würzburg, Germany
yuuya.sugita@gmail.com

Jun Tani
RIKEN Brain Science Institute
2-1 Hirosawa, Wako-shi, Saitama 3510198, Japan
tani@brain.riken.jp

Martin V. Butz
Department of Psychology III (Cognitive Psychology)
University of Würzburg
Röntgenring 11, 97070 Würzburg, Germany
butz@psychologie.uni-wuerzburg.de

Running Head: Emerging Compositional Braitenberg Codes

Corresponding Author: Yuuya Sugita

Phone: +49-176 38 40 85 39

FAX: Sorry, not available.

Abstract

Although many researchers have suggested that compositional concepts should be sensorimotor grounded, how this may be accomplished remains unclear. This paper introduces a second-order neural network with parametric biases (sNNPB) that learns role-argument structures of the concepts based on sensorimotor time series data. The data was produced by a simulated robot that executes distinct object interactions (move-to and orient-toward). We show that various sNNPB setups can compositionally imitate object-interactions, which were not necessarily trained. We furthermore show that these imitation capabilities are accomplished by a compositional task representation in the PB values, by the generation of suitable task-oriented, Braitenberg-like sensory encodings in hidden sensory layers, and by the PB-dependent, interaction-specific, selective activation of these sensory encodings. These internal representations structure themselves rather independently of the utilized sensory input and motor output codes. Thus, we hypothesize that second order connections may be essential to drive the learning of both sensorimotor-grounded compositional structures and Braitenberg-like, behavior-oriented "propresentations". From a cognitive perspective, we show how sensorimotor time series may be processed to generate the signals necessary to ground a compositional system of concepts.

1 Introduction

Compositionality and similarity are often assumed to involve different cognitive processes. Similarity is considered to be sensory- and possibly motor-grounded. It may lead to the formation of perceptual feature-based categorizations. Compositionality, on the other hand, refers to the more abstract, "cognitive" capability of handling symbols, for which proper role-argument structures need to be available. The role-argument structures specify how symbols are related systematically based on their semantic roles to form whole complex concepts. Barsalou (1999) proposed that symbols may be grounded in perceptions by means of simulators and simulations. The representation of the role-argument structure was represented in the notion of *frames*. How these frame may be learned by an organism, however, remains an open question.

In contrast to this position, this study explores a continuous developmental path from similarity to compositionality by means of an example-based concept formation approach. We trained a simulated robot equipped with a second-order neural network with parametric biases (sNNPB) on analog sensorimotor time series data. In particular, the robot was taught to either move to or orient itself toward a colored object, where the orienting behavior could be further modified by a directional offset. Teaching proceeded by demonstrating particular interactions, indicating their distinctness from other interactions. The resulting sensorimotor patterns were used to train an sNNPB by means of standard back-propagation. It is shown that the network develops compositional interaction concepts solely due to the training setup, the modular sNNPB architecture, and the sensory- and motor-capabilities of the simulated robot. In more detail, we show that the visually-driven side of the network yields behavior-oriented goal encodings that essentially provide distributed Braitenberg-like signals (Braitenberg, 1984). The activity in the PB neurons then selectively combines those signals that generate the desired interaction pattern. These observations suggest that the setup fosters the generation of goal-oriented, anticipatory behavioral encodings, which are known to be highly beneficial for cognitive agents (Butz and Pezzulo, 2008).

In conclusion, we propose that the sNNPB network generates encodings that may be found in the dorsal and ventral processing pathways of the brain. The dorsal pathway provides robot-relative, goal-oriented interaction signals (Holmes and Spence, 2004) leading to goal-oriented motor encodings (Graziano, 2006) – it is mimicked by our sensory-to-motor pathway in the sNNPB. The ventral pathway, on the other hand, provides object identities (Riesenhuber and Poggio, 2000) and leads to the selection of currently desired environmental interactions given currently available object affordances in the sense of Gibson (1979). While we do not implement the object identification part, the PB-to-motor pathway in the sNNPB mimics the selection of a currently desired object interaction.

We now first give background on the challenge to gain semantic compositionality based on similarity measures alone. Next, we introduce the simulated robot architecture, the neural network architecture, and the different settings evaluated. After that, we provide a detailed performance and sNNPB structural analysis verifying emergent semantic compositionality and emergent Braitenberg codes. Finally, we conclude the paper with a general discussion.

2 Similarity and Compositionality

One of the most severe difficulties in constructivist accounts of concept formation is the origin of the compositional role-argument structure of concepts (cf. Markman and Dietrich, 1999). The origin of compositionality should be attributed to the interaction between cognitive processes and sensorimotor experiences – unlike nativist models, which assume innate compositional representations (cf. e.g. Fodor and Lepore, 2002). For example, the representational rewriting (RR) theory proposed by Karmiloff-Smith (1992) suggests that compositional concepts are acquired through the "re-writing" of pre-acquired holistic sensorimotor concepts. First, a young infant may conceptualize his or her sensorimotor experiences by rote, which cannot be related to other concepts. At this level, no skill transfer is possible due to the lack of connections amongst the concepts. Later, these holistic concepts may be translated into compositional concepts. How this may be accomplished, however, has not been clarified, yet. This study investigates how holistic concepts may be related to each other to yield compositional concept structures. The most important modification of the original idea is that holistic concepts are related to each other by innate similarity measures. Thus, we address the questions of (1) how similarity may be implemented innately; and (2) how this innate similarity may be transformed into compositionality.

We hypothesize that similarity may be implemented innately by the embodiment of the agent with its continuous sensorimotor dynamics, including the involved learning mechanisms. Consider a simple case about color similarity. The similarity of colors can be defined in a behavior-oriented manner without referring to analytical features of colors such as HSV value, RGB value, or wavelength. It is plausible to consider, for example, that an animal perceives 560nm stimuli as being similar to 550nm stimuli when the animal generates a reaction associated with 550nm stimuli in the context of previously unseen 560nm stimuli. In this way, similarity of colors may be defined based on observed equivalences in performance transfer rather than solely based on analytical features. The more complex perceptions and behavioral interactions are, the more relevant similarity measures based on such behavioral transfer are expected to become. For example, similarities between motor skills may be defined in terms of how much the training of one skill improves another skill. In our study, similarity measures depend on the predefined sNNPB architecture, the format of its input and output, and the learning conditions.

Two counter-intuitive aspects of such transfer-based similarity should be noted. First, symmetry of the transfer-based similarity is not guaranteed, namely, B is not always "similar" to A even if A is similar to B. This possible asymmetry is actually observed in cognitive preferences (Tversky, 1984). For example, we prefer "A scanner is like a copy machine" to "A copy machine is like a scanner." Second, transfer-based similarity can vary depending on given training constraints. This is similar to a peak shift of a generalization curve, which is, for example, observed in perceptual generalizations (Hanson, 1959). Note also that transfer-based similarity is possibly multidimensional although dimensions are not defined explicitly. For example, green can be similar to both yellowish-green and dark green in terms of a proper transfer-based similarity as well as an analytical similarity based on predefined multidimensional representation such as RGB value.

The "structural alignment" hypothesis proposed by Gentner and Markman (1997) considers how innate similarity may be transformed into compositionality. They consider similarity and analogy to be two extremes on a continuum and suggest that the comprehension of surface similarity may facilitate the understanding of concept structures, which is essential for analogical transfer. Base on these idea, Gentner and Markman (1997) proposed a computational mechanism called "structural alignment," which is commonly used to explain similarity-based and analogical transfer. Analogical transfer usually refers to the knowledge transfer across problems of different domains such as between fluid dynamics and electromagnetics. Their discussion, however, is also applicable for compositionality, which refers to knowledge transfer across smaller domains. However, the computational model of Gentner and Markman (1997) relies on predefined compositional representations, essentially adopting analytical similarity to compare two problems. For example, two interactions may be considered similar based on their common representational constituents, which are predefined. In this work, structural alignment will be reconsidered from a constructivist view, replacing analytical similarity with transfer-based similarity, which is grounded in behavioral performance emitted by the learning agent.

3 Robot System Setup

Our robot setup is based on a psychological experiment conducted by Meltzoff (1988b), who examined the conceptualization ability of pre-linguistic infants. The original study reported that 9-month-old infants could imitate previously unseen object-manipulating actions for 24 hours after the presentation of the actions. This indicates that pre-linguistic infants memorize the presented actions in an abstracted representation, which provides a foundation of later language acquisition (Meltzoff, 1988a).

In our experiment, the setup is modified in order to focus on the emerging process of concept formation. Actions are presented by steering a robotic subject by means of a teaching program. The robot perceives its own visual input and motor output during the presentation of the teaching examples. Thus, the necessary translation between allocentric and egocentric views is omitted. On the other hand, the time scale of the experiment is expanded, including the acquisition of the structured representation since the robot needs to develop role-argument frames for representing the encountered interactions by examples.

3.1 Robot and Environment

We now give details on the robot-environment setup in the experiments as well as on how the sensorimotor time series data was generated. The simulated robot consisted of a simple two-wheeled robot platform that was equipped with visual surround sensors. The body of the robot was a cylinder of 24cm diameter and 14cm height. The visual sensors were located at the center of the body (in simulation) and partitioned the covered 120° view into nine uniform areas for which the sensors reported the dominant color and the color-covered size.

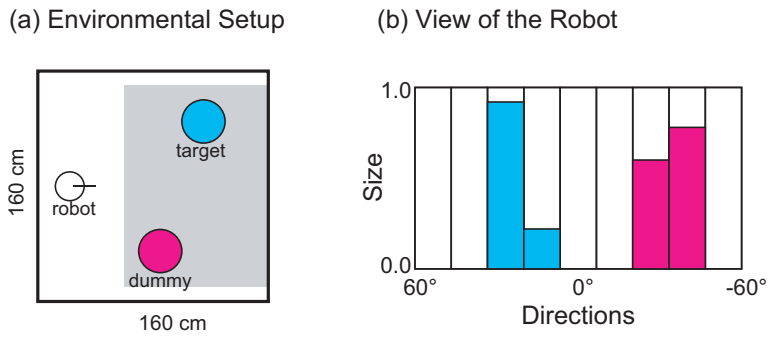

Figure 1: The robot starts with a fixed starting position. A target and an optional dummy colored object are placed randomly within the shaded area (W120cm × D134cm) shown in (a). The robot takes a vision input shown in (b) in this environmental situation.

In each trial of an interaction, the robot interacts with one of six colored cylinders (`blue`, `cyan`, `green`, `yellow`, `orange`, and `magenta`) of 13cm diameter and 25cm height in the environment where one or two objects, one of which is the target, are randomly placed, as shown in Fig. 1. The interactions are classified into 36 categories: either of two types of object interactions are executed: `moveto` (move to) or `orientto` (orient toward) one of the six targets. In the `moveto` interactions, the robot moves toward the target and stops just before touching it. In the `orientto` interaction, the robot must orient itself toward the target by rotating its body. The `orientto` interaction additionally takes one of five modifiers, which designate an angular offset of the final orientation with respect to the target: (`-30`, `-18`, `0`, `+18`, and `+30`). A negative angle indicates an offset to the left. In the following, the interaction is denoted as a concatenation of labels of one of the types, one of the targets, and, optionally, one of the offset angles; for example, `orientto-blue+18`. In some situations, `orientto` with one of the offsets, e.g `orientto+18`, is regarded as a particular interaction type. It should be noted that the labels are used for convenience only – the robot never perceives any explicit information about the semantic structure of the interactions.

Six independent blocks of learning experiments were conducted with supervised data of different sparseness, each of which contained 1, 1, 4, 4, 7 and 21 out of the 36 sorts of possible interactions, as shown in Fig. 2, respectively. We present these six supervised blocks to illustrate the robot's conceptualization capabilities, including similarity and compositionality biases. Each experimental epoch consists of three phases: creation of training data, learning, and evaluating the imitation performance on all possible interaction types.

3.2 Generation of Training Data

To gather sensorimotor time series data, the robot was controlled by a training program. For each goal-oriented behavioral interaction, 120 training sequences were generated

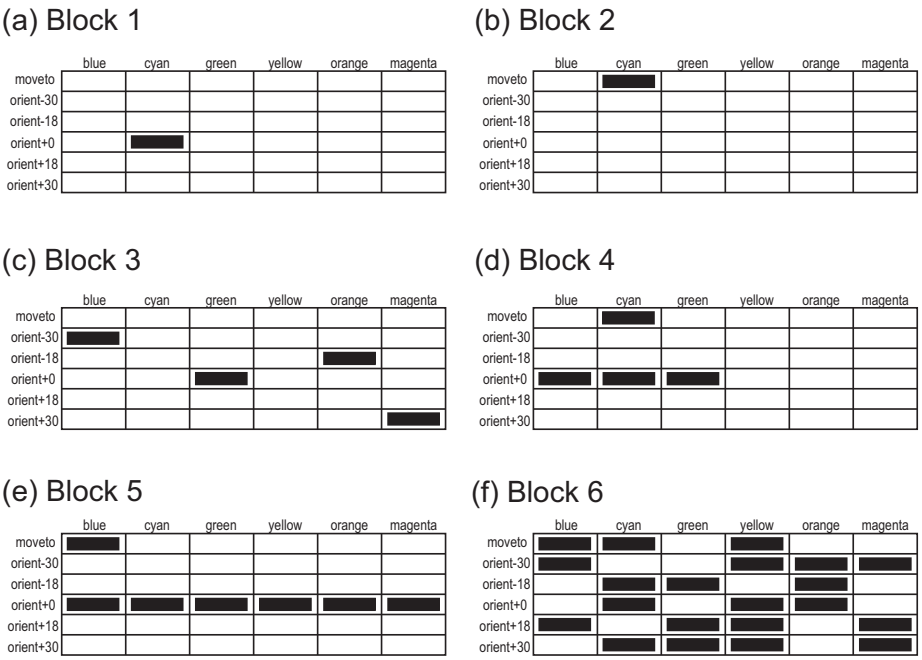

Figure 2: Distribution of trained sets of interactions for each experimental block

in different environmental settings. In 20 out of the 120 cases, only a target object was placed in the environment, and in the remaining 100 cases, a dummy object was placed in addition to the target object. The dummy object was chosen from among five objects other than the target, and 20 examples were recorded for each object.

Representing the distance r[cm] and the direction θ[rad] of the target object, the program generates motor commands that are appropriate for executing a particular interaction. The motor command specifies the velocities of two wheels (v_L[cm/step], v_R[cm/step]). In particular, the program instructs `moveto` interactions by moving the robot to a distance of 35.0cm from the target object as follows:

$$v_R = \max(-1.0, \min(v_\theta + v_r, 1.0)) \tag{1}$$

$$v_L = \max(-1.0, \min(-v_\theta + v_r, 1.0)) \tag{2}$$

$$v_\theta = \begin{cases} 0.25\theta & \text{if } r \geq 36.0, \\ 0.75\theta & \text{otherwise,} \end{cases} \tag{3}$$

$$v_r = \begin{cases} 0.0045r + 0.158 & \text{if } r \geq 36.0, \\ 0.0045(r - 35.0) & \text{otherwise.} \end{cases} \tag{4}$$

Similarly, a program instructing `orientto` interactions calculates motor commands with a given offset angle ϕ as following:

$$v_R = \max(-1.0, \min(0.5(\theta - \phi), 1.0)), \tag{5}$$

$$v_L = -v_R. \tag{6}$$

While the teaching program thus had precise information about the target object and task, the sNNPB architecture received only simulated visual information, as specified above.

3.3 Evaluating Imitation Capability

After the learning, the robot is tested to what extent it can imitate each of the 36 possible interactions including unfamiliar ones. At the beginning of each examination epoch, the sNNPB is fed with 12 examples of a certain interaction to set the PB activity. Next, the network is required to imitate these interactions in 280 different test environments. The success rates of all interactions are recorded for later analysis. The successful imitation is judged in terms of the final relative distance and direction to a given target. The robot is required to keep the designated conditions for 100 consecutive time steps within 250 time steps. In order to accomplish the `moveto` interactions, the robot had to stay within 40.0 cm from the target without touching it. For the `orientto` interactions, the robot was required to orient itself toward the designated direction within an error of $\pm 6^\circ$.

4 Second-Order Neural Network with Parametric Biases

We report experiments with three sNNPB setups. We now first specify the network architecture that was common to all three setups and then specify the distinctions be-

tween the different setups.

4.1 Network Architecture

The architecture of the implemented sNNPB is shown in Fig. 3. The network consists of two interacting sub-networks: a feed-forward sensor-to-motor network (*stm-net*), whose connectivity is modified by a meta-level network (*meta-net*).

The stm-net is depicted on the left-hand side of the figure. It takes as input the visual information at vision input (VI) layer from the simulated camera. Next, it transforms this information via two hidden layers – the hidden layer (H) and the resulting processed visual representation layer (VR) in the following way:

$$\mathrm{VR}_i(t) = f_{\mathrm{VR}}\left(\sum_{j=0}^{N_{\mathrm{H}}} w_{\mathrm{VR}(i)\leftarrow\mathrm{H}(j)} \cdot \mathrm{H}_j(t)\right), \quad \mathrm{H}_i(t) = f_{\mathrm{H}}\left(\sum_{j=0}^{N_{\mathrm{VI}}} w_{\mathrm{H}(i)\leftarrow\mathrm{VI}(j)} \cdot \mathrm{VI}_j(t)\right), \tag{7}$$

where we denote the activity of a node by X_i ($X \in \{\mathrm{MO}, \mathrm{VR}, \mathrm{H}, \mathrm{VI}\}$), the connection weights between two nodes by $w_{X_i\leftarrow Y_j}$, the time step by t, and the non-linear transformation function by f_X (a hyperbolic tangent).

Finally, the information contained in VR is transferred to the motor output layer (MO), which generates the velocities of the two wheels of the robot by:

$$\mathrm{MO}_i(t) = \sum_{j=0}^{N_{\mathrm{VR}}} \mathrm{sC}_{i,j} \cdot \mathrm{VR}_j(t), \tag{8}$$

where $\mathrm{sC}_{i,j}$ specifies the weights generated in the second order connections as specified below. The stm-net is thus a conventional layered feed-forward neural network, except for that it has second-order connections (Pollack, 1990) between the VR and MO layers, meaning that the weights between VR and MO are flexibly set to particular values. This enables the stm-net to generate different sensorimotor interactions, dependent on the currently activated weights from VR to MO.

The weights of the second-order connections are determined by the meta-net shown on the right side of Fig. 3. The meta-net itself is also a conventional feed-forward neural network. It takes as input a concept vector of parametric biases (PB) and generates the weights of the second-order connections by means of the activity in the second-order connectivity (sC) layer.

$$\mathrm{sC}_{i,j} = f_{\mathrm{sC}}\left(\sum_{k=0}^{N_{\mathrm{PB}}} w_{\mathrm{sC}(i,j)\leftarrow\mathrm{PB}(k)} \cdot \mathrm{PB}_k\right), \tag{9}$$

where sC_{ij} is the output of a node in the sC layer, which corresponds to a connectivity from the j-th VR node to the i-th MO node.

The generation of action outputs works as follows. First, a concept vector $\mathbf{u}_i$ needs to be available, which is used to set the PB node activities. This vector then determines the values of the sC connections according to (9). These connections are set once at the beginning of an interaction episode and are kept fixed while a particular

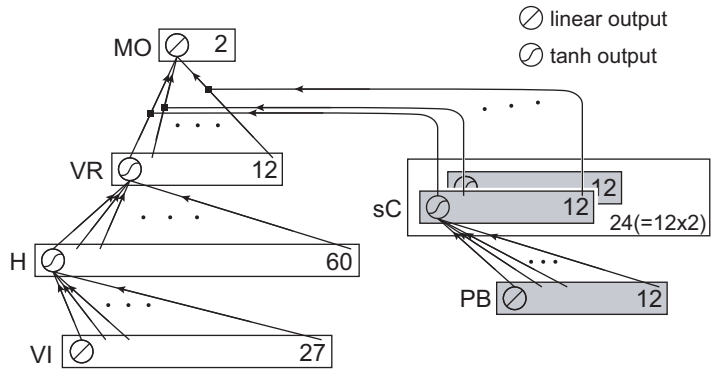

Figure 3: **The sNNPB architecture:** A rectangle represents a layer, which contains multiple nodes. The number of nodes and the utilized output function are indicated in each rectangle. The meta-net, which consists of the gray layers, controls the connectivity from the VR to the MO layer.

interaction unfolds. To generate actual motor outputs, sensory activities are then transferred into motor output activities according to (7 and 8). Note that the time scale of the meta-net is thus different from the stm-net. The 'normal' connection weights $W = \{w_{\mathrm{H}\leftarrow\mathrm{VI}}, w_{\mathrm{VR}\leftarrow\mathrm{H}}, w_{\mathrm{sC}\leftarrow\mathrm{PB}}\}$ capture the common characteristics among all of the provided interactions $\mathcal{I}'$, whereas each concept vector $\mathbf{u}_i$ determines particular second order connections sC to realize particular object interactions $i \in \mathcal{I}'$.

4.2 Learning

Unlike a standard layered neural network, not only connection weights W but also the interaction-respective concept vectors $\mathbf{u}_i$ ($i \in \mathcal{I}'$) are optimized in the sNNPB, where the vectors are stored in $U = \{\mathbf{u}_i \mid i \in \mathcal{I}'\}$. Both sets of parameters are optimized simultaneously by means of the conventional steepest descent method with respect to the output error defined as follows:

$$E(W^T, U^T) = \sum_{i\in\mathcal{I}'} E_i(W^T, \mathbf{u}_i^T) \tag{10}$$

$$E_i(W^T, \mathbf{u}_i^T) = \sum_{j=0}^{N_i} \sum_{t=0}^{l_{ij}} E_{ij}(t; W^T, \mathbf{u}_i^T) \tag{11}$$

$$E_{ij}(t; W^T, \mathbf{u}_i^T) = \|\hat{MO}_{i,j}(t) - MO(t; W^T, \mathbf{u}_i^T)\|^2, \tag{12}$$

where T denotes the current learning iteration, W^T the current connection weights, U^T the set of interaction concept vectors, $\mathbf{u}_i^T (\in U)$ a particular interaction concept vector to be optimized, $N_i (= 120)$ the number of pre-recorded training examples of the i-th interaction concept, l_{ij} the length of the j-th time series example of the i-th interaction,

$\hat{MO}_{i,j}(t)$ the desired motor activity of the time series with respect to its corresponding visual input $\hat{VI}_{i,j}(t)$, and $MO(t; W^T, \mathbf{u}_i^T)$ the actual output of the network at that time.

The learning procedure is implemented by using the conventional back-propagation algorithm. At the beginning, all the connection weight values W^0 are initialized with uniformly distributed random values $\in [-0.1, 0.1]$, and all entries in each $\mathbf{u}_i^0 \in U^0$ are set to zero. Each learning example indicates its particular interaction concept correspondence i, which leads to the re-application of the corresponding current concept vector $\mathbf{u}_i^T$ and the according adjustment of that vector. Thus, learning errors are back-propagated to their corresponding concept vectors $\mathbf{u}_i$. In all the reported experiments below, we conducted 30,000 learning iterations. Alg. 1 specifies the learning procedure precisely.

Algorithm 1 Learning procedure in sNNPB.

for all interaction i in $\mathcal{I}'$ **do**
  Load the stored $\mathbf{u}_i^T$ to the PB layer.
  for all pre-recorded examples j of the interaction i **do**
    Calculate the delta errors of connection weights $-\partial E_{ij}/\partial W$ and of PB vector $-\partial E_{ij}/\partial \mathbf{u}_i$ by using the back-propagation algorithm
  end for
  Sum up the delta errors over all time steps t of all time-series (i, j) to obtain $\delta \mathbf{u}_i^{T+1}$.

$$\left(\because \delta \mathbf{u}_i^{T+1} = -\frac{\partial E}{\partial \mathbf{u}_i}(W^T, U^T) = -\frac{\partial E_i}{\partial \mathbf{u}_i}(W^T, \mathbf{u}_i^T)\right).$$

  Update $\mathbf{u}_i$ as follows:

$$\Delta \mathbf{u}_i^{T+1} = (1 - \eta_u) \cdot \Delta \mathbf{u}_i^T + \eta_u \cdot \delta \mathbf{u}_i^{T+1}, \tag{13}$$

$$\mathbf{u}_i^{T+1} = \mathbf{u}_i^T + \alpha_u \cdot \Delta \mathbf{u}_i^{T+1}, \tag{14}$$

  where α_u and η_u are learning coefficient and momentum, respectively.
end for
Sum up the delta errors of W for all time steps t of all the time-series j of all trained interaction $i \in \mathcal{I}'$ to obtain δW^{T+1}.

$$\left(\because \delta W^{T+1} = -\frac{\partial E}{\partial W}(W^T, U^T)\right).$$

Update W as follows

$$\Delta W^{T+1} = (1 - \eta_w) \cdot \Delta W^T + \eta_w \cdot \delta W^{T+1}, \tag{15}$$

$$W^{T+1} = W^T + \alpha_w \cdot \Delta W^{T+1}, \tag{16}$$

where α_w and η_w are the learning coefficient and momentum, respectively.

4.3 Recognition and Imitation

The goal of the sNNPB is to re-produce – or imitate – particular object interactions including unfamiliar ones. To test this capability, we simulate a recognition and an imitation process for all the 36 possible interactions $i \in calI$. In the recognition process, the sNNPB is presented with 12 examples of particular sensorimotor interaction i, which are conceptualized into a concept vector $\mathbf{u}_i$ by means of error back-propagation, as used during learning (Alg. 1). The error is back-propagated to the PB neurons, where the averaged error determines the recognition vector. Connections weights W are not updated making this process computationally more effective. Essentially this method induces the re-usage of existing repertoires rather than the modification of them. The recognition vector $\mathbf{u}_i$ is then applied in other robot-object scenarios and tested for its general capability to imitate specific object interactions i.

4.4 Three Network Training Setups

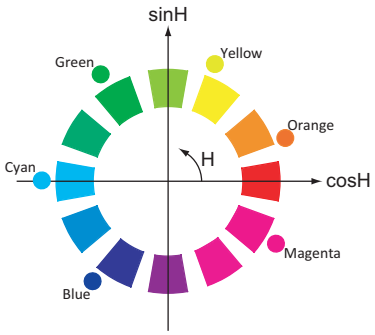

Figure 4: **Colors of the objects**

We examine three different variations of the sNNPB. For the basic network, the visual input is encoded in a 27-dimensional vector. The visual field is vertically segmented into nine regions. Each region is represented by the fraction of the region covered by colored patches and the dominant hue of the patches in the region. The hue H is encoded by the position $(\cos H, \sin H)$ in the color circle shown in Fig. 4. Motor output is encoded as a 2-dimensional vector representing velocity of left and right wheels, each of which is a real value ranging from -1.0 to 1.0. A negative value indicates reverse rotation.

The two networks other than the basic one have a modified VI layer and MO layer, respectively. The VI-modified network has 36 VI nodes since the dominant color of each visual region is provided in the RGB format. The MO-modified network has 10 MO nodes, where the velocity of each wheel is encoded by a 5-dimensional vector. The vector represents the velocity v in the form of:

$$G(v) = [f(-0.6; v), f(-0.3; v), f(0.0; v), f(0.3; v), f(0.6; v)],$$

where $f(x; v)$ is a Gaussian distribution $N(x; \mu = v, \sigma^2 = 0.3^2)$. In either cases, the sensorimotor encoding is different from the basic case but *local* similarity is preserved. Motor similarity defined by the Gaussian and linear encodings are locally identical since Euclidean distance between Gaussian-encoded velocities $\|G(v_2) - G(v_1)\|$ is almost proportional to $\|v_1 - v_2\|$ if $\|v_1 - v_2\|$ is sufficiently small. For the same reason, sensory similarity defined by Hue and RGB encodings are locally identical, too.

5 Behavioral Generalizations

This section presents results regarding the obtained behavioral imitation performance. First, we focus on the generalized imitation capabilities achieved depending on the distribution of trained interactions (cf. Fig. 2) and given sensory and motor encodings (see Sec.4.4). Next, we analyse the generated behavioral mappings over the possible sensory input ranges.

5.1 Skill Generalization and Recombination

In the following, we progressively increase the number of trained interactions and analyze the compositionality of the behavioral generalizations achieved. For each trained interaction block (cf. Fig. 2), three sNNPBs were trained with different network connectivity initializations. Next, untrained interactions were tested by first deriving a maximally suitable PB activity by means of back-propagation (see Sec.4.3) and then testing that PB activity on 280 other object setups, as detailed in Sec.3.3.

5.1.1 Learning from one Interaction Only

In block 1, the robot was only trained on `orientto-cyan+0` interaction examples. Figure 5 shows that the acquired skill is transferred across offsets and targets to some extent for all three setups. No transfer across interaction types (that is, from `orientto` to `moveto`) is realized, however. The closer color of target and offset of the interaction are, the higher the imitation success rate. The strength of the transfer, however, depends on the given setup. In the RGB-based color encoding case, the transfer across targets is slightly weaker but it extends slightly further to other color encodings, somewhat reflecting the neighborhood relations of the RGB color space (Fig. 5(a) versus Fig. 5(b)). Similarly, transfer across offsets is more limited in the Gaussian motor encoding case (Fig. 5(a) versus Fig. 5(c)). The non-linearity induced by the Gaussian motor encoding makes it difficult to find common skills, such as convergent dynamics, among the `orientto` interactions with different offsets.

In block 2, the `moveto-cyan` interaction was trained. In the linear motor encoding cases shown in Figs. 6(a) and (b), transfer across types of interactions, from `moveto` to `orientto`, is observed, as well as additional offset transfer and color transfer. Thus, convergent dynamics that are acquired by learning `moveto-cyan` are reused to generate `orientto-cyan`. However, the successful transfer depends on the chosen motor encoding, as hardly any transfer is observable in the Gaussian motor encoding case (c.f. Fig. 6(c)). This shows that while the Gaussian encoding does not diminish learning

(a) Hue + Linear

	blue	cyan	green	yellow	orange	magenta
moveto	00	00	00	00	00	00
orient-30	09	04	24	12	13	12
orient-18	06	45	20	07	11	12
orient+0	33	89	33	07	07	02
orient+18	21	56	53	07	10	08
orient+30	16	17	33	14	10	14

(b) RGB + Linear

	blue	cyan	green	yellow	orange	magenta
moveto	00	00	00	00	00	00
orient-30	15	16	26	15	09	09
orient-18	09	49	23	24	13	09
orient+0	22	99	21	14	06	05
orient+18	30	20	31	31	10	10
orient+30	16	05	29	14	06	07

(c) Hue + Gaussian

	blue	cyan	green	yellow	orange	magenta
moveto	00	00	00	00	00	00
orient-30	02	00	05	09	07	06
orient-18	03	23	09	14	08	03
orient+0	36	91	60	09	06	03
orient+18	44	21	22	03	02	05
orient+30	36	02	08	08	06	09

Figure 5: **Imitation performance obtained in block 1:** Local offset and color generalizations within the `orientto` interaction space. Success rates of imitation are co-encoded by number and color. Instructed interactions are surrounded by a black frame.

success, skill-transfer across types is disrupted because the transfer requires non-local, color-sensitive generalizations and prevents the direct linear combination of rotation and forward movement signals.

(a) Hue + Linear

	blue	cyan	green	yellow	orange	magenta
moveto	38	87	35	07	03	09
orient-30	05	02	02	03	04	15
orient-18	14	18	04	02	02	07
orient+0	35	80	14	02	00	00
orient+18	05	15	13	01	01	01
orient+30	21	30	07	01	01	03

(b) RGB + Linear

	blue	cyan	green	yellow	orange	magenta
moveto	42	89	33	00	00	18
orient-30	39	20	05	03	04	08
orient-18	41	64	18	03	01	07
orient+0	39	85	16	12	00	05
orient+18	04	11	21	06	04	03
orient+30	09	03	14	05	12	05

(c) Hue + Gaussian

	blue	cyan	green	yellow	orange	magenta
moveto	29	90	31	04	01	00
orient-30	24	25	05	00	00	01
orient-18	14	11	13	01	01	01
orient+0	02	03	19	03	03	01
orient+18	01	00	08	03	02	01
orient+30	01	00	01	01	02	01

Figure 6: **Imitation performance obtained in block 2:** Generalizations from `moveto` to `orientto` interactions.

We like to emphasize the observed asymmetric skill-transfer from `moveto-cyan` to `orientto-cyan` but not vice versa. This is the case due to the behavioral asymmetry between `moveto` and `orientto` interactions: `moveto` requires additional approaching skills that are not necessary for `orientto`. Both, however, require a kind-of pivoting skill, which is blend into the approaching skill in `moveto` interactions. Back-propagation apparently identifies the PB components that control the approach-

ing behavior and thus can inhibit those selectively to realize the untrained `orientto` behaviors. From a cognitive perspective, this result replicates empirical asymmetry of similarity comparisons (Tversky, 1984) without providing explicit, innate compositional representations.

5.1.2 Compositionality when Learning From Multiple Interactions

Albeit combinatorial skill-transfer is still restricted when training four different `orientto` interactions (cf. Fig. 7), color-respective as well as offset-respective sensorimotor generalizations are clearly observable. Results of RGB-based color encoding cases are omitted from now on, because all tests yielded generally comparable results to the Hue-based color encoding.

Recombinations of interactions are obtained clearly in block 4, where four interactions are instructed in a systematic manner (cf. Fig. 8). The robot could imitate two unfamiliar interactions `moveto-blue` and `moveto-green` at a much higher success rate than in block 2, where only transfer across the target contributed. Thus, while the `orientto` skill cannot produce the `moveto` skill itself, its color-sensitive orientation component can be diverted into the `moveto` skill – effectively increasing the success rate for the two neighboring `moveto` interactions. This skill transfer can only be explained by a recombination of interactions. It suggests that a sub-symbolic equivalence of the following symbolic compositional system was acquired:

$$\langle Interaction \rangle ::= \oplus(\langle Type \rangle, \langle Target \rangle), \tag{17}$$

$$\langle Type \rangle ::= \texttt{moveto} \mid \texttt{orientto}, \tag{18}$$

$$\langle Target \rangle ::= \texttt{blue} \mid \texttt{cyan} \mid \texttt{green}, \tag{19}$$

where $\langle Interaction \rangle$ is a set of concepts representing generable interactions, and $\langle Type \rangle$ and $\langle Target \rangle$ are a set of elemental concepts representing types of interactions and targets, respectively. A composition rule, which combines a type and a target into a whole interaction, is denoted as $\oplus$.

(a) Hue + Linear

	blue	cyan	green	yellow	orange	magenta
moveto	00	00	00	00	00	00
orient-30	87	26	52	26	75	38
orient-18	73	26	69	42	80	45
orient+0	27	40	81	24	70	36
orient+18	14	21	72	21	43	59
orient+30	26	29	58	29	43	90

(b) Hue + Gaussian

	blue	cyan	green	yellow	orange	magenta
moveto	00	00	00	00	00	00
orient-30	93	26	18	19	39	16
orient-18	20	04	09	10	93	41
orient+0	12	21	92	34	39	22
orient+18	10	16	63	29	13	05
orient+30	08	09	34	18	50	94

Figure 7: **Imitation performance obtained in block 3:** Generalizations over color and offset concepts within the `orientto` interaction space.

An even stronger compositional recombination can be observed in block 5 (Fig. 9(a)). The skills acquired by learning the `moveto-blue` interaction transferred to the five other `moveto` interactions. This transfer was not obtained in the Gaussian motor encoding case (Fig. 9(b)). If, however, the full `orientto` interaction space was trained

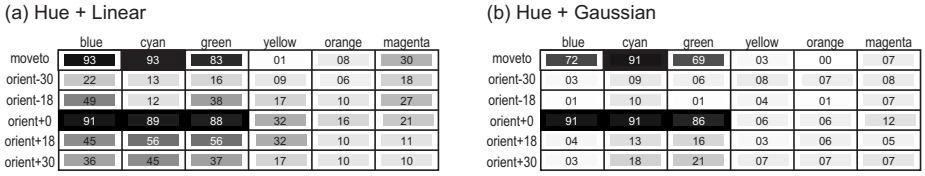

Figure 8: **Imitation performance obtained in block 4:** Local, color-respective generalizations from `orientto` to `moveto` interactions.

and, for example, the `moveto-blue` interaction, then color-respective transfer also occurs in the Gaussian motor encoding case (not shown). Thus, broadly reusable skills can be organized even if predefined (motor) surface similarity is highly non-linear.

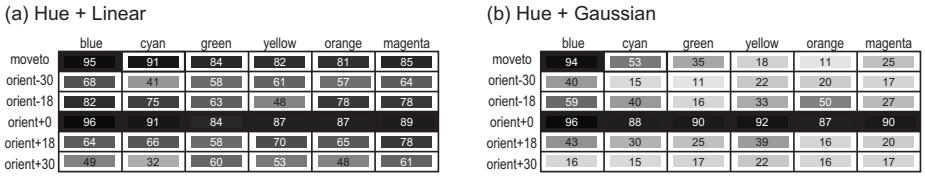

Figure 9: **Imitation performance obtained in block 5:** Color-respective generalizations from `orientto` to `moveto` interactions.

5.1.3 Acquisition of All Interaction Skills

Finally, the robot could imitate all the possible interactions well when it learned 21 out of the 36 interactions, as shown in Fig. 10. For this result, the robot apparently developed the following fully compositional system of concepts:

$$\begin{aligned} \langle Interaction \rangle &::= \oplus_1(\texttt{moveto}, \langle Target \rangle) \\ &\quad | \quad \oplus_2(\texttt{orientto}, \langle Target \rangle, \langle Offset \rangle), \\ \langle Target \rangle &::= \texttt{blue} \mid \texttt{cyan} \mid \texttt{green} \mid \texttt{yellow} \mid \texttt{orange} \mid \texttt{magenta}, \\ \langle Offset \rangle &::= \texttt{-30} \mid \texttt{-18} \mid \texttt{0} \mid \texttt{+18} \mid \texttt{+30}, \end{aligned} \tag{20}$$

where $\langle Interaction \rangle$ is a set of concepts representing the available interactions, and $\langle Target \rangle$ and $\langle Offset \rangle$ are a set of elemental concepts representing a target and an offset, respectively. Composition rules for the two types of interactions, `moveto` and `orientto`, are denoted as $\oplus_1$ and $\oplus_2$. The sub-symbolic implementation of this concept system will be analyzed in detail in the subsequent sections.

5.2 Generalized Behavioral Patterns

While the previous section showed that the network is able to generalize its interaction skills in a functionally compositional way, we now focus on how the necessary interac-

(a) Hue + Linear

	blue	cyan	green	yellow	orange	magenta
moveto	98	97	98	97	90	85
orient-30	78	77	76	80	80	76
orient-18	76	81	86	76	86	75
orient+0	74	88	92	87	88	74
orient+18	89	76	88	89	74	89
orient+30	73	75	83	85	75	89

(b) Hue + Gaussian

	blue	cyan	green	yellow	orange	magenta
moveto	95	96	95	93	87	88
orient-30	91	83	82	85	89	91
orient-18	92	93	94	84	93	89
orient+0	89	96	97	96	95	93
orient+18	96	94	95	95	87	95
orient+30	82	93	91	93	81	93

Figure 10: **Imitation performance obtained in block 6:** Both encodings yield a generalization performance above 73%.

tion behavior is generated and generalized to untrained interactions. We are interested in the extent to which the sNNPB generalizes the sensorimotor mappings beyond the cases it was trained on and thus focus on the replication of and generalization over the object interactions generated by the training program (cf. (1 – 6)). The presented data in this sections were generated in block 6 by using an sNNPB in the Hue-based, linear encoding setup.

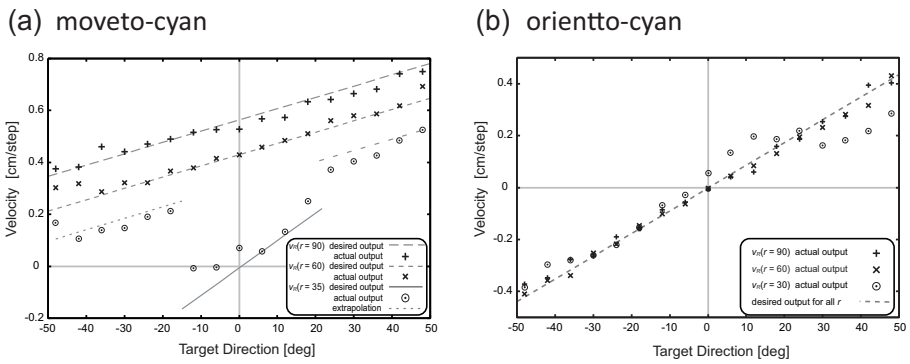

Figure 11: Task-specific direction and distance to velocity mappings.

Figures 11(a,b) show the acquired mappings between the relative direction and distance of a target object and the velocity of the right wheel for `moveto-cyan` and `orientto-cyan`, respectively. The motor output is determined in environments where only one `cyan` object was located. The figures show that the robot can reconstruct the position-velocity mapping for both the `moveto-cyan` and the `orientto-cyan` interactions. An interesting generalization can be observed for the `moveto-cyan` case when the robot is located close to the object ($r = 35$). In this case, the robot was only trained on cases where the object was within 15° relative directional range due to the environmental setup (see Fig. 1). While the desired output is well-approximated within that range, outside of that range the system extrapolates to the cases where the object is further distant. The actual velocity then follows a line labeled "extrapolation" in Fig. 11(a), which is obtained by applying $r = 35$ to the equations for $r \geq 36$ (cf. (3 and 4)).

Besides this generalization to visual input ranges that were not learned, Fig. 12 shows that sNNPB actually also learned to *avoid* currently undesirable objects. Figure 12(a) shows the hue dependency of motor output v_R for the `orientto-cyan` interaction concept[1]. The output was recorded by presenting 40 different colored objects at 19 different positions 90cm distant from the robot. At the hue corresponding to the cyan object (hue $\approx 180°$), it can be seen that the robot's right wheel rotates forward when a cyan object is located to the right of the robot but backwards when the object is located to the left, thus replicating the trained sensorimotor interactions. However, if a different colored object is observed given the `orientto-cyan` instruction, this pattern is increasingly reversed, thus increasingly avoiding other objects the stronger their color differs from cyan. Thus, the robot generalized over the color space.

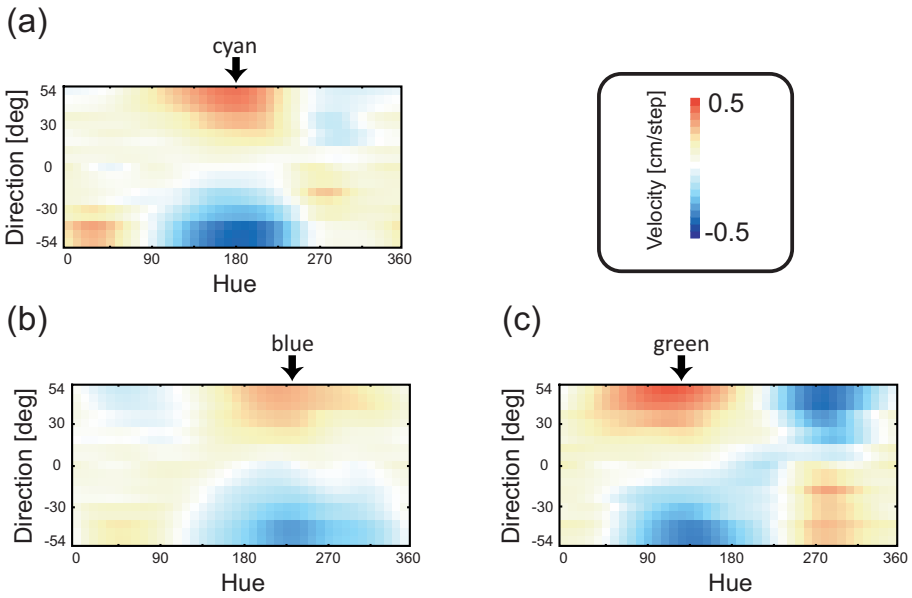

Figure 12: Hue-direction to velocity mappings for specific `orientto` interactions.

Similar patterns can also be observed for other target colors (figures 12(b,c)). It should be noted, however, that `orientto-blue` was never instructed during the learning phase. Further analyses revealed that all six `orientto-`τ interactions share a highly similar mapping with different displacements corresponding to the color of the target object τ. This indicates that some common internal mechanisms are reused among all the `orientto-`τ interactions and are modified based on the currently desired target τ, as specified in the PB layer.

Another repetitive motor pattern should be found with respect to the directional offset ϕ, which modified the object-respective turning behavior according to (5, 6). In Fig. 13, the five lines show the velocity profiles computed from (5) with the trained

[1]The motor output v_L was generally mirrored to the one of v_R in this case (not shown).

offsets. The actual direction-velocity mappings for `orientto-cyan` with offsets confirm the existence of the common mechanism. The mappings are obtained under the condition that the `cyan` object is placed at 90cm away from the robot. Note that the two interaction concepts `orientto-cyan-30` and `orientto-cyan+18` were never instructed during the learning phase. Each of the mappings follows its desired profile. Also, systematic error patterns can be observed from the profiles – again suggesting common mechanisms that realize the offset-respective mappings.

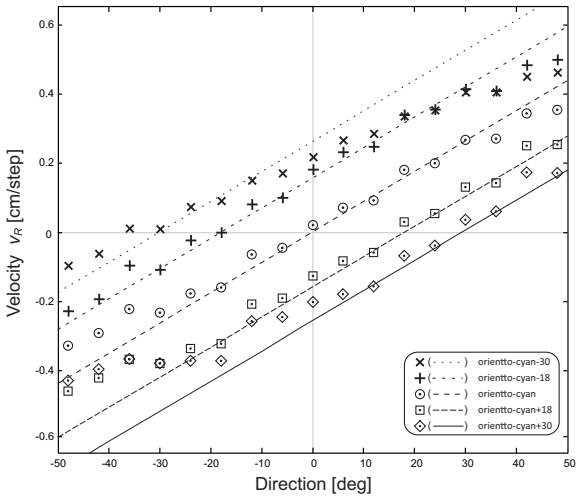

Figure 13: Direction-velocity map for different offset angles

In sum, we were able to show (a) behavioral generalizations with respect to hue space, (b) emergent avoidance behavior that has only been trained indirectly, and (c) behavioral generalizations in terms of offset value inter and extrapolations.

6 Network Structure Analysis

While the behavioral analyses in the last section confirmed that there is an inherent pressure to structure the sensorimotor interaction skills in a compositional way, it remains unclear how the network encodes this compositionality and how it generates the sensorimotor interaction patterns. Thus, we now analyze the sNNPB encodings in more detail. First, we analyze the structure of the PB layer and show that a subsymbolic equivalence of compositional role-argument structures emerged. Next, we reveal *how* these compositional structures in the PB layer realize the invocation of the sensory-to-motor mappings that are necessary to realize a particular interaction. Finally, we analyze the behavior-oriented structures in the VR layer (cf. Fig. 3).

6.1 Functional Compositionality in Concept Space

Seeing that the sNNPB can yield behavioral recombination, we now first turn to the PB layer and investigate how the interactions are represented in a "compositional" manner. Thus, we structurally analyze the PB space, as defined by the interaction-respective concept vectors $\mathbf{u}_i$ for all the 36 possible interactions $i \in \mathcal{I}$. The presented structures in this sections were generated by an sNNPB in the Hue-based, linear encoding setup. Comparable structures were obtained by using the other encoding setups.

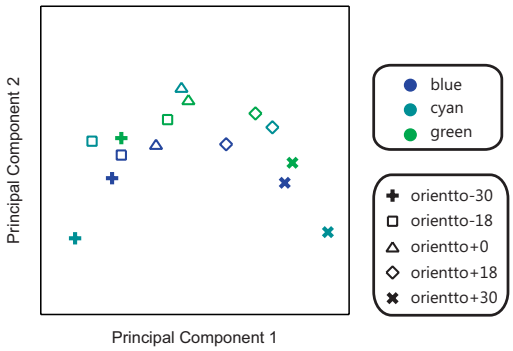

Figure 14: **Concept structure obtained in block 1:** Mainly sensorimotor similarities are observable.

Figure 14 shows concept structures obtained in block 1. The shown 15 concept vectors represent `orientto` interactions toward either of `blue`, `cyan`, or `green` objects with five the different possible offsets. The vectors are projected into a surface spanned by the first and second principal components of the 30 concept vectors for the `orientto`-τ-ϕ interactions. The six `moveto`-τ concept vectors were removed from this principal component analysis, since they took aberrant values. The accumulated contribution rate of the two principal components was 0.77. With regard to the presented 15 interactions, similar interactions are arranged nearby in the concept space. Moreover, a rudimentary continuum of interactions by offset is observed in a horseshoe shape. However, no regular sub-arrangements are observed, suggesting that the information of target color and offset angle was not clearly separated by the sNNPB. This implies that every `orientto` interaction with different offsets employs its proprietary target representation. This is consistent with the observed behavioral performance in the last section: no recombination of interactions was observed.

In block 6, in contrast, a systematic geometric arrangement self-organized among all the 36 concept vectors, as shown in Fig. 15. The top four principal components of all 36 concept vectors are presented in the figure, re-arranged by means of an affine transformation for visualization convenience. The accumulated contribution rate of the first four principle components was 0.78. The arrangement consists of three sub-arrangements, which correspond to the three roles constituting the interactions: $\langle Type \rangle$, $\langle Target \rangle$, and $\langle Offset \rangle$ (cf. Equation 20). In Fig. 15(a), the interactions are clustered with respect to its type, `moveto` or `orientto` along y-axis. In the `orientto` cluster,

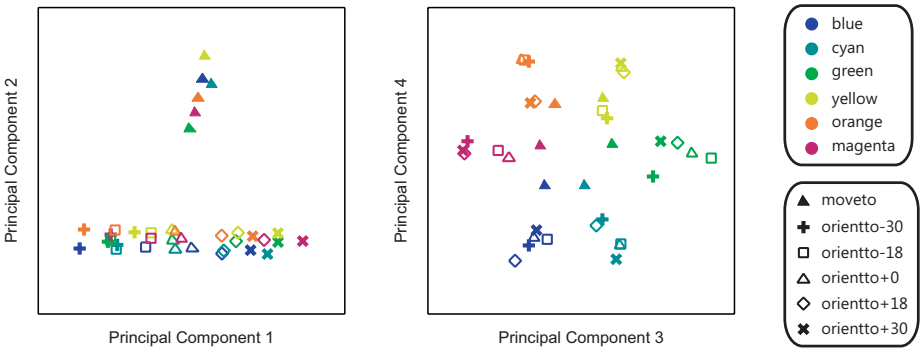

Figure 15: **Concept structure obtained in block 6:** Full semantic compositionality is observable.

five sub-clusters are found for each of the offsets although they overlap to some extent. These five sub-clusters constitute a linear continuum of `orientto` interactions by offset along the x-axis. In Fig. 15(b), six clusters correspond to each of the target colors. Furthermore, the clusters are arranged in a circle comparable to the continuum of color by hue (see Fig. 4). Note that the three role-relevant sub-spaces are orthogonal to each other. Due to the orthogonality, elemental concepts are reusable in all the possible combinations. Thus, we discover an underlying analog mechanism of the role-argument structure estimated in Sec.5.1.3 and specified in (20) by considering the following correspondences:

1. The roles $\langle Type \rangle$, $\langle Target \rangle$, and $\langle Offset \rangle$ correspond to the sub-spaces, respectively;
2. The elemental concepts for each role, for example, `orientto`, `blue`, and `-30`, are vectors pointing to the center of gravity of the corresponding clusters;
3. The argument structure, which combine the elemental concepts, is implemented by the disjoint union of the corresponding vectors.

Further analyses have shown that intermediate arrangements can be found in other blocks. Thus, a continuous process underlying the transition from similarity to compositionality can be conceived in terms of the geometric arrangements among the concept vectors.

6.2 Selecting and Modifying Sensorimotor Mappings

So far, we have shown that the PB space expresses compositional interaction concepts by representing $\langle Type \rangle$, $\langle Target \rangle$, and $\langle Offset \rangle$ in role-specific subspaces. Since the interaction concept vector determines the mapping from VR to MO (cf. Fig. 3), we now investigate *how* these compositional vectors may activate the appropriate sensorimotor mapping. Thus, the crucial questions are: (a) how can the connection weights $sC_{i,j}$

suitably select the appropriate sensory-to-motor mappings and (b) how is the sensory information transformed in layer VR to enable the weight-driven selection mechanism. We answer these questions in this and the following subsections, respectively.

Our results essentially suggest that the connection weights $sC_{i,j}$ realize the target selectivity by a sinusoidal distribution pattern over the color space with respect to particular $\langle Type \rangle$ and $\langle Offset \rangle$ interactions. To be more precise, we denote particular interaction concept weights by $sC_{i,j}^{\mu\tau\phi}$ with $\mu\tau\phi \in \mathcal{I}$ and interaction type $\mu \in \{\texttt{orientto}, \texttt{moveto}\}$, target $\tau \in \{\texttt{orange}, \texttt{yellow}, \texttt{green}, \texttt{cyan}, \texttt{blue}, \texttt{magenta}\}$, and offset $\phi \in \{-30, -18, 0, 18, 30\}$. Considering the color-respective hue values as input, we approximate the six color-specific weight values along the hue axis with a sinusoidal equation, that is, given a particular interaction type μ, we approximate the weight values $sC_{i,j}^{\mu\tau\phi}$ by the following function:

$$a_{ij} \cdot \sin(\psi_\tau - b_{ij}) + c_{ij} \;\; \texttt{with} \;\; c_{ij} = A_{ij}\phi + B_{ij}, \tag{21}$$

where ψ_τ denotes the corresponding hue of the respective targets τ. Amplitude a_{ij} and phase offset b_{ij} determine how one full sinusoidal period is positioned over the hue input space. The fitting curves are obtained by using the conventional Levenberg-Marquardt method.

Figure 16 shows the fitted amplitudes a_{ij}, phase offsets b_{ij}, and function offsets c_{ij} respective the six action-modified interaction concepts for all 12 nodes ($j = \{0, 1, \cdots, 11\}$) of the VR layer connecting to the right-wheel neuron ($i = 1$) of the MO layer. Figure 17 additionally shows exemplar sinusoidal mappings as well as the node-respective multiple correlation values of the respective mappings. The suffixes of the fitted parameters are omitted from now on.

Several observations can be made. First, nodes #1 and #8 show low correlation values and consistently very low amplitude values. Thus, these two nodes do not fit into the proposed scheme. We show below that these nodes indeed provide nearly color-independent object distance signals. Additionally, nodes #3 and #7 also show rather low correlation values and low amplitudes, which however strongly differ with respect to the different offsets. Thus, we consider those nodes intermediate nodes, which are somewhat color-sensitive but also yield distance-sensitivity. However, the other eight out of twelve nodes exhibit high amplitudes and correlation values. Moreover, the phase offset values b are very similar in these nodes over all five modifications of the `orientto` action.

Also the `moveto` actions employ somewhat similar sinusoidal patterns. The phase offsets b are generally similar to the ones for the `orientto` interactions, suggesting a similar approach to combining VR activities for the motor output generation. The amplitude values are generally smaller than the ones for the `orientto` interactions. This seems to be highly plausible, since less rotation is necessary in the `moveto` action but additional forward movement needs to be superimposed. Only node #3 shows a higher amplitude, suggesting a special relevance for that object interaction. Finally, the function offsets indicate (Fig. 16(c)) the strong general relevance of nodes #1, #3, and #8 for the `moveto` interactions, compared to the `orientto` interactions. Note also that only for these three nodes, the offset is similar for the mapping to the right wheel and the left wheel, corroborating evidence that these three nodes control the forward

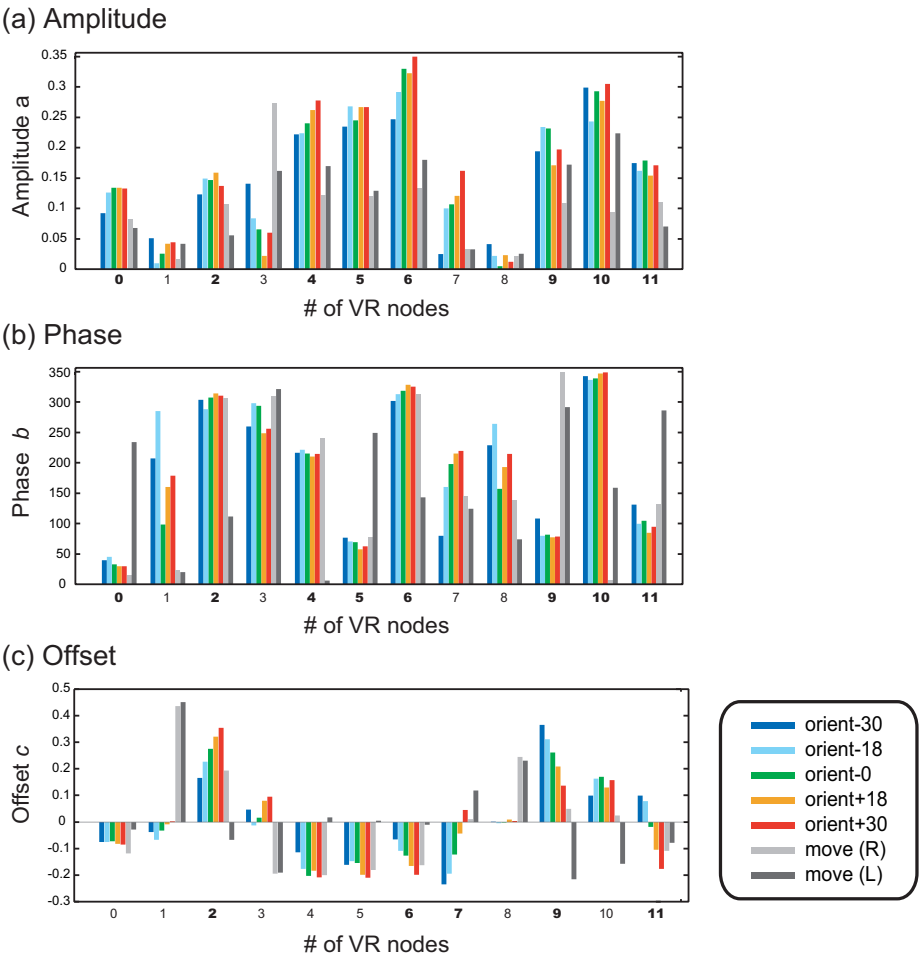

Figure 16: Amplitude (a), phase offset (b), and function offset (c) of each VR nodes for the six interaction concepts (five `orientto` interactions and the `moveto` interaction): Fitted parameters for the connections to a right-wheel neuron and both right- and left-wheel neurons are presented for the five `orientto` and the `moveto` interactions, respectively. Target-relevant nodes are highlighted in (a) and (b). Offset-relevant nodes are highlighted in (c).

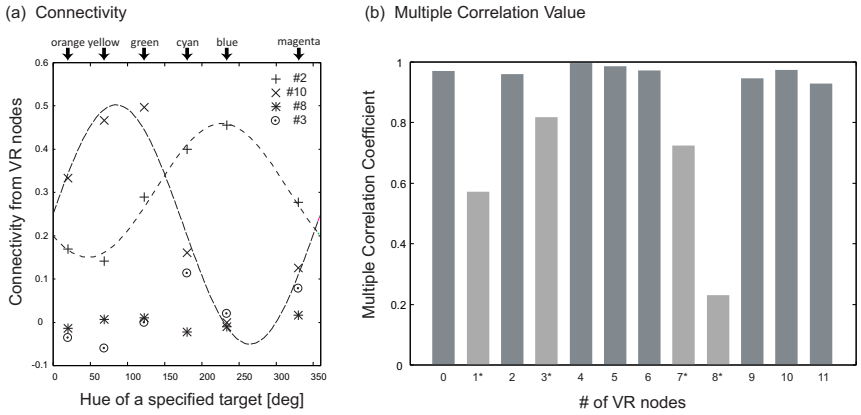

Figure 17: **(a) Connectivity from** VR **nodes to the motor output nodes that generates the velocity of the right wheel; (b) multiple correlation values between actual and approximated connectivity:**

movement.

At the same time, the VR nodes are categorized differently in terms of the relevance to the determination of final angular offsets. Strong correlation is observed between the above-mentioned fitting parameter c and a given offset angles ϕ for six VR nodes. Figures 18(a – c) show linear regression results of c in terms of the fitting function $A\phi + B$ where A and B are fitting parameters defined in (21). Examples of fitting curves are presented in Fig. 18(a) for two offset-relevant nodes #2 and #9 and an offset-irrelevant node #10. The categorization is obtained in terms of the proportional constant A and multiple correlation values, as shown in Figs. 18(b) and (c), respectively. The five strongly offset-relevant nodes are fitted with proportional constant ($|A| > 0.002$) and with multiple correlation values higher than 0.98. Also the offset values of the sinusoidal equation illustrate this correlation (cf. Fig. 16(c)). It may come as a surprise that the gradients of nodes #2 and #7 are positive while the gradients of nodes #6, #9, and #11 are negative, however. This suggests that inverted visual information should be contained in the respective VR nodes.

6.3 Reusable Components of Sensorimotor Mappings

The above analysis has shown that the sNNPB utilizes a sinusoidal selection mechanism that determines the relevance of particular VR nodes for particular color-object interactions. An additional value offsets the sinusoidal curves to scale their mapping influence offset-specific. What remains to be shown is how these selective weight influences lead to the realization of the observed behavior. The question thus is, which information is actually encoded in the VR nodes to control the unrolling of the desired sensorimotor interaction patterns? Originally, we expected that this layer would provide visually-processed factual information about the surrounding environment, such

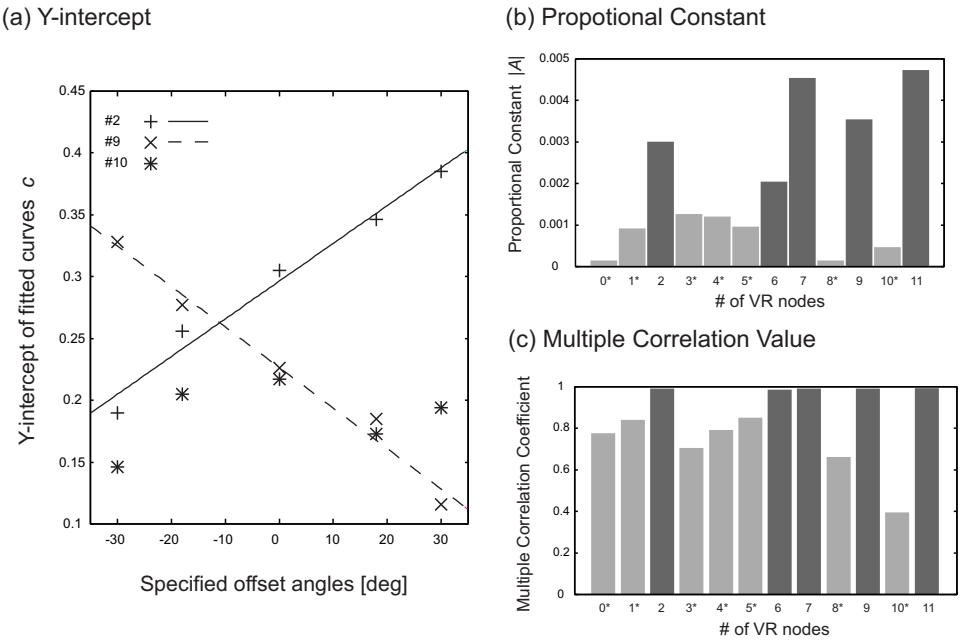

Figure 18: Correlation between c and offset angle

as "orange-object at 45° and blue-object at −30°." However, it turns out that this layer actually provides behavior-oriented information about the surrounding objects in the form of Braitenberg-like goal-oriented sensory encodings that is properly combined by means of the $sC_{i,j}$ weights to yield the appropriate interaction patterns.

We first analyze nodes #1 and #8, which were identified as `moveto`-relevant nodes in the PB-dependent connectivity analysis. The activation level of #1 decreases gradually as any object comes closer, as shown in Fig. 19. Meanwhile, the activation of #8 changes suddenly when any object comes just in front of the robot as shown in Fig. 20. This confirms that these two nodes provide suitable distance codes that can be recruited by the `moveto` interactions. The more negative the activity in these two nodes is, the lower the speed of the two wheels. Due to the strong non-linear sensitivity of node #8 around 35cm with a switch from positive to negative values, the sNNPB realizes the stopping-behavior. Essentially, the nodes encode Braitenberg-like distance information enabling the mapping from object distance to wheel speeds.

When combining the VR activities of the remaining ten nodes, we receive the following patterns: sensorimotor mappings of `orientto` interactions are composed of three components, a *common component*, which is shared by all the `orientto` interactions with any offset angle, a *target-relevant component*, and an *offset-relevant component*. The common component is obtained based on the term B of the sinusoidal function (21). Figure 21(a) shows a sensorimotor mapping that consists of the ten VR nodes with an activity ratio of each node given by Bs. This component is almost

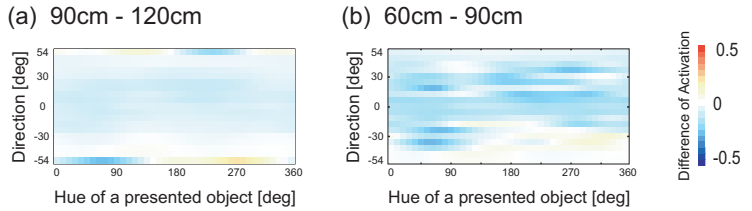

Figure 19: **Activation of** VR **node #1:** Sensitivity of VR node #1 to the distance to an object is shown as differences of two outputs for the object placed at 90cm and 120cm, 60cm and 90cm away from the robot.

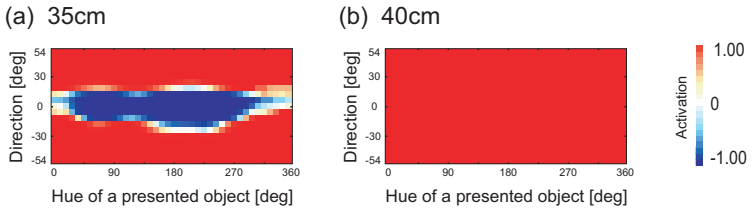

Figure 20: **Activation of** VR **node #8:** the output of VR node #8 is recorded when an object are placed at 35cm and 40cm away from the robot.

insensitive to hue, but contributes slightly to convergence to any object with no offset.

The target-relevant component is obtained as a combination of the eight hue-relevant VR nodes (#0, #2, #4, #5, #6, #9, #10, #11) with the ratio given by averaged a and b values over all offset angles. This component produces a suitable linear gradient from positive to negative values. Figures 21(c1 – c3) show that the zero activity hits the spot at the zero offset nearly perfectly for the respective target objects. Moreover, the pattern increasingly reverses for colors that increasingly differ from the target color. Thus, the above-mentioned shifting of the sensorimotor mappings (cf. Fig. 12) is explained in terms of this component: the processed visual information provides the suitable gradients. The encoding can be regarded as the provision of perfectly task-suited, color-sensitive Braitenberg sensors: for each target color there are two sensors whose activity is maximal given the target color and decreases toward negative values with increasingly different hue-encoded colors. Positioning these sensors with a sufficient perceptual radius to the front-left and -right of the robot, the difference yields approximately exactly the gradient map as shown in Figs. 21(c1 – c3).

Finally, the offset-relevant component is obtained as a combination of the offset-relevant VR nodes (#2, #6, #7, #9, and #11) with the ratio given by $A\phi$. This component is almost flat and contributes to changing the convergent direction by levelling the velocity uniformly as shown in Fig. 21(b). Thus, for each offset-value, the sensorimotor mapping is uniformly shifted to the position where the transfer from positive to negative wheel speeds and vice versa should take place. This encoding actually suggests the

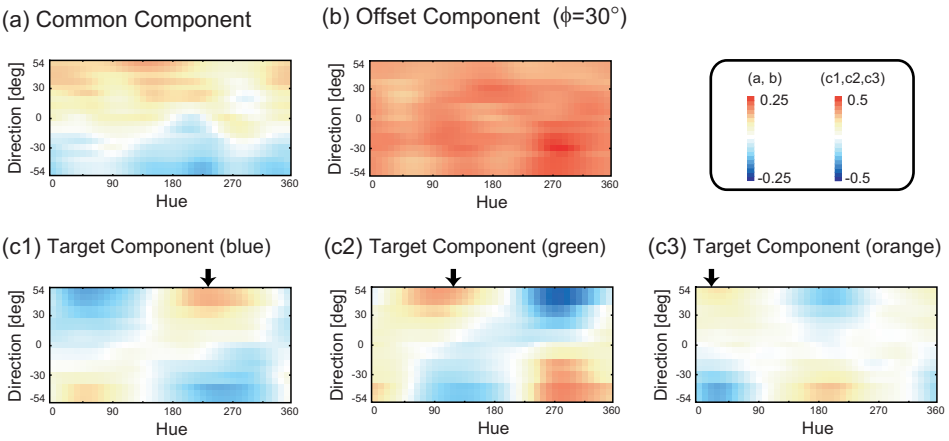

Figure 21: **Reusable Components of sensor-motor maps for `orientto` interactions: A common component shared by all `orientto` interactions (a), an offset-relevant component (b), and a target-relevant component (c1, c2, c3) are presented.**

invention of a necessary constant offset value, which can produce constant offsets over the whole sensory space[2].

To see how the visual information is combined to achieve these mappings, we show the output patterns of the other ten nodes of the VR layer in Fig. 22. The output of the VR nodes was recorded by presenting 40 different colored objects at 19 different positions 90cm distant from the robot. Further analysis reveals that the activation of all ten nodes is approximated as a sinusoidal function of hue of a presented object H for particular directions (that is, sinusoidal patterns along x-Axis for particular directions). These sinusoidal patterns were observed irrespective of color encodings of the visual input nodes: either using $(\sin H, \cos H)$ (cf. Fig. 22) or (r, g, b) (not shown). Thus, the offset-respective sinusoidal patterns of VR nodes along the hue axis, in conjunction with sinusoidal patterns generated in the $\mathrm{sC}_{i,j}$ connections (cf. Sec.6.2), enable the color selectivity and the observed behavioral generalization over the color space. The linear gradient comes into being by the PB-controlled combinations of local, color-offset specific linear gradients. These can be observed for given color encodings along the y-Axis in the nodes of Fig. 22, where the observable single non-linearities (switch from positive to negative gradient or vice versa) are blended into each other to generate an approximate linear wheel-speed mapping (cf. Figs. 21(c1-c3)). Thus, the color-relevant VR nodes provide a mixture of color- and direction-sensitive sensors that do not encode object locations explicitly, but rather encode object directions color-respectively.

[2]Surprisingly, experiments with bias nodes in the VR layer showed that back-propagation fails to recruit those nodes for the offset control but still "invents" its own offset encoding as explained above.

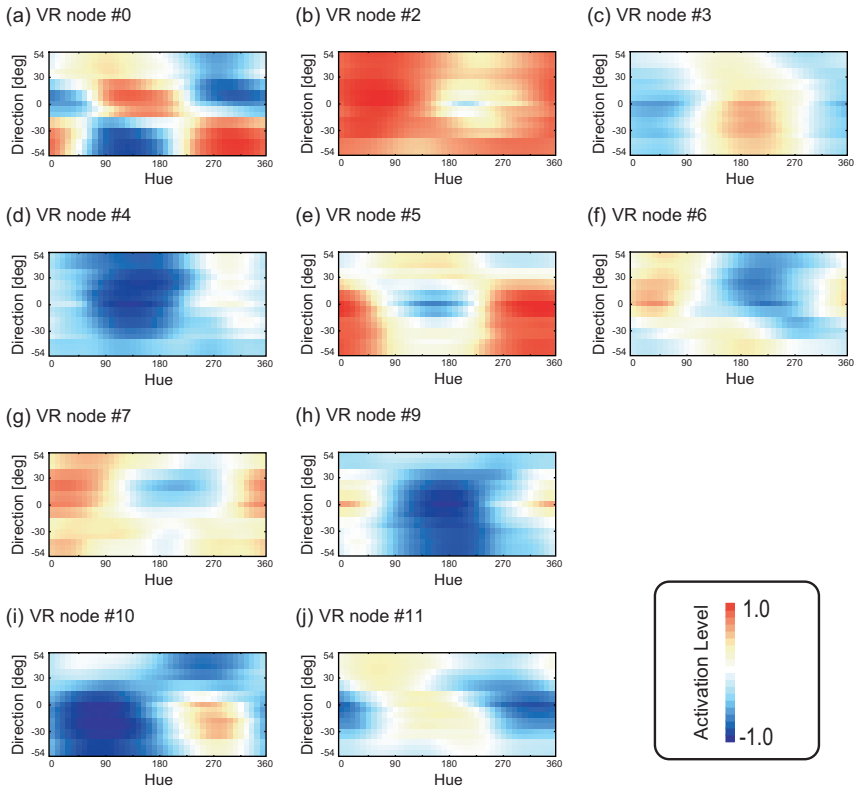

Figure 22: Activation patterns of VR nodes

7 Discussion

7.1 Relational View of Functional Compositionality

Previous works have attempted to bridge the gap between analog sensorimotor experiences and a compositional system of discrete concepts. Karmiloff-Smith (1992) proposed intermediate *level-I* representations. A level-I representation is characterized as an implicit procedural knowledge that is acquired by rote-learning a particular sensorimotor event. The level-I representation is thus analogous to the sensorimotor experience. On the other hand, it does not provide any essential mechanisms to rewrite itself into compositional concepts, since it is completely *unstructured*.

In contrast, image schemas, which were proposed by Johnson (1987) and Lakoff (1987), are easily connected to compositional concepts because they consist of mutually related parts. In this way, they can capture recurring *structural* patterns of our sensorimotor experiences. However, the sensorimotor mechanisms that underlie the formation of such image schemas are still controversial. It is essentially puzzling how image schemas may be derived from sensorimotor experience but meanwhile may be

a prerequisite for organizing experiences, as pointed out by Clausner (2005). Thus, at least a principle to organize sensorimotor experiences may be required, if a compositional system should be acquired based on sensorimotor experiences (cf. Mandler, 1992).

As an alternative, our study shows that structural alignment can take place in a sensorimotor-grounded, analog concept space. By associating individual (initially unstructured) concept vectors with particular interactions during learning, the learning algorithm forms progressively more compositional representations, which enable the combinatorial transfer of skills. Thus, functional compositionality is realized due to the sensorimotor-grounded, relational structures among the concepts. This relational view makes it possible to transform similarity into (functional) compositionality, as was shown in the structural transformations from the ones in Fig. 14 to the ones in Fig. 15.

In addition, the natural interdependency among semantic roles is preserved inevitably in the learning approach where interactions are conceptualized without explicit decomposition. Note that each semantic role cannot exist by itself. For example, consider the concept $\oplus(\texttt{moveto}, \texttt{blue})$, which consists of two concepts that play the roles of an interaction type and a target, respectively. Both depend on each other since the target is something that the robot interacts with and the interaction type is a way to handle the target. Thus, it is impossible to conceptualize `blue` as a target without referring to any interaction types. An analogy may be the fact that it is impossible to define the function of a pawn meaningfully without referring to other chess pieces (de Saussure, 1986). Consistently with this property, both semantic roles need to emerge simultaneously in the concept space.

Fig. 23 shows an idealized concept structure that was approximately emerging in block 6 of our experiments. Both target and offset subspaces are presented. As explained above, the roles are realized in terms of geometric regularity. A sub-symbolic equivalence of the target role are the alignment of five *aligned* circles (or hexagons), which are congruent and parallel to each other. Similarly, the offset role is shown as six aligned solid lines. We like to stress that both congruences accompany each other inherently since it is impossible to generate aligned substructures in one subspace without generating any aligned substructures in the other space. It is also important that the argument structure emerges as the orthogonal nature between the two subspaces at the same time. This explanation can be extended to the full concept space that was acquired in the experimental block 6, where target, type, and offset roles depended on each other in a similar manner (cf. Fig. 15).

7.2 Distinctness for Functional Compositionality

Sub-symbolic models that acquire embodied compositional concepts are also proposed by Cangelosi and Riga (2006) and Tuci, Ferrauto, Massera and Nolfi (2010). Instead of the PB layer, both models employ symbolic input layers, which specify interaction concepts that are to be acquired or generated. Each symbolic node corresponds to a particular predefined *elemental* concept. The actual interaction concept is specified by the combination of two or more active nodes. Thus, their models find internal configurations that plug sensorimotor experiences of a robotic agent into predefined concept

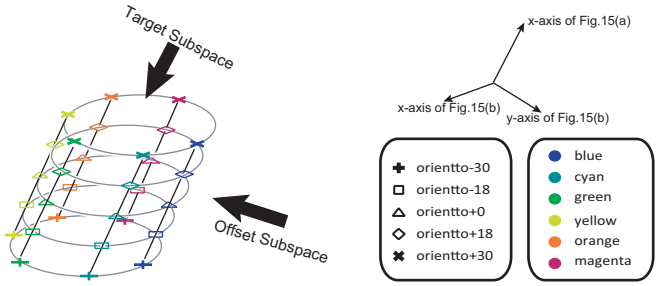

Figure 23: **An idealized concept space:** Four out of three dimensions of concept structure acquired in block 6 are illustrated.

structures. In contrast, our model acquires emergent compositional concept structures solely by the provision of distinctness indicators for the trained interactions. Thus, this learning constraint does not restrict the obtainable concept structures to predefined ones.

Our previous model (Sugita and Tani, 2005) utilized linguistic structure as a compositional pressure on behavioral conceptualization in a different manner from the above-mentioned two models. A recurrent neural network with parametric biases (Tani, Ito and Sugita, 2004) was employed to learn multiple different interactions. The provided linguistic pressure introduced geometric regularities into the behavioral concept space, which made the holistic interaction concepts accessible from the linguistic side. Thus, no behavioral skill transfer was observed. Note that this result is very different from the presented study although they looks similar in term of the acquired concept space.

In the current sNNPB architecture, compositional goal-oriented interaction encodings are fostered because the correlations between target positions and motor outputs form interaction-specific equivalence classes. However, the sensorimotor similarity alone would not bootstrap the categorization of the interactions because sNNPB has no innate mechanisms for focusing on the target. In other words, the predefined vision encoding provides behavior-irrelevant similarity, which depends on positions of both target and dummy objects equally. Neither does the categorization emerge due to the motor time series data alone because the motor data strongly vary within a particular interaction dependent on the presented object constellations. Thus, the provided distinctness information about the trained interactions enabled the network to learn to focus on the target, using a sinusoidal encoding approach. Vision encodings are re-organized in a behavior-relevant manner by means of the Braitenberg-like, color-separating sensory encodings (cf. Fig. 22), which provides the reusable components of sensorimotor mappings (cf. Fig. 21).

8 Summary and Conclusion

In this paper we have shown that a second-order neural network with parametric biases (sNNPB) can learn sensorimotor-grounded, semantic compositional structures.

This was achieved by the very general back-propagation learning algorithm plus the provided distinctness (but not compositional) information for each distinct interaction trained. Selectively activated, the compositional structures could produce particular object interactions on demand. The compositional structures were realized by two interdependent modules: the meta-net produced compositional second-order connection weights while the stm-net produced processed sensory information again with a compositional, task-oriented structure. The latter encoding can be regarded as a compositional Braitenberg code, because it allows the compositional activation of those sensory information sources that are task-relevant and that can be linearly mapped onto motor codes. The fact that neural activity in the VR layer did not linearly correlate with object locations, furthermore suggests that the setup induced pro-motor sensory encodings, rather than compression-oriented representational encodings. Thus, we can conclude that the sNNPB network architecture produced an encoding that transferred motor and sensory similarity into effective compositional structures.

Further analyses showed that compositionality was realized by a representation that is based on a sub-symbolic geometric arrangement. This regular geometric arrangement interactively self-organizes interdependent semantic roles in separate principal component axes. The experimental results suggest that a whole concept does not need to be decomposed into its assumed constituents explicitly. In fact, we believe that an explicit decomposition may prevent the acquisition of situated compositional systems because the enforced abstraction restricts the compositionality and thus may prevent the formation of further reaching similarities within the enforced compositional structures. In contrast, the situatedness of the compositional elements in our model is assured by learning the most suitable compositional, geometric structure that is able to selectively activate distinct sensory-to-motor interaction mappings. Thus, we refrained from an enforced symbolization, but succeeded in grounding compositionality in sensorimotor codes alone.

While our achievements suggest that semantic compositionality can be generated by means of second-order connections plus distinctness information about the trained interactions alone, future work will need to refine the current approach in several respects. First, it is somewhat unsatisfactory that the distinctness information is provided by the teacher. We believe that distinctness information may come either from internal motivation and reward signals or from linguistic signals. In a previous study, two of the authors (Sugita and Tani, 2005) had succeeded in associating the PB structure of the behavioral control module with another PB structure in a linguistic module. We intend to pursue this research further – however, now with the sNNPB introduced here. If properly linked, then the self-organizing behavioral PB structure works as a pre-linguistic concept structure, which facilitates later syntax acquisition (cf. Dominey, 2006).

Second, the model should be extended to acquire recursively structured interaction concepts. The recursive structure can be represented as a fractal geometric arrangement in principle, as shown in Nishimoto and Tani (2004); Sugita and Butz (2010). A learning model in which the fractal structure self-organizes through the learning of sensorimotor time series involving behaviors of an agent may be investigated in this respect.

Finally, to foster the scalability of the system to more diverse and complex interactions, we believe it will be necessary to further modularize the learning architecture

and to introduce more explicit mechanisms of focus and attention. As was shown, the system learned to focus on a particular target interaction by employing sinusoidal, goal-oriented encodings. While this encoding was an unexpected, rather innovative invention of the sNNPB, to be able to separate sensory information further and to temporary focus on the interaction-relevant one, more explicit sensory filtering mechanisms will most likely be necessary. For example, Gaussian Mixture Models have been employed to identify the crucial interaction constraints in particular robot arm object interactions (Calinon and Billard, 2009). Similar approaches may be useful to enable the more explicit selective activation of goal-oriented interaction foci. However, to achieve this, the further modularization of sensory and motor encodings is expected to be necessary. Only redundant, sensory, motor, and sensorimotor encoding structures are expected to enable the selective identification of those pieces of information that are crucial for the realization of particular interactions. Thus, clearly the grand challenge for future research is to learn compositional encodings in more general environmental setups with a more capable robotic interaction system. The insights gained by the current work suggest that the second-order control of mappings from suitably processed, pro-motor encoded sensory information to motor control codes may play a crucial role in achieving this endeavour.

Acknowledgement

This study is supported by Grants-in-Aid for Scientific Research (No. 20700188) from the Japan Society for the Promotion of Science (JSPS).

References

Barsalou, L. (1999). Perceptual symbol systems. *Behavioral and Brain Sciences*, 22:577–600.

Braitenberg, V. (1984). *Vehicles: Experiments in Synthetic Psychology*. MIT Press, Cambridge, MA.

Butz, M. V. and Pezzulo, G. (2008). Benefits of anticipations in cognitive agents. In Pezzulo, G., Butz, M. V., Castelfranchi, C., and Falcone, R., editors, *The Challenge of Anticipation: A Unifying Framework for the Analysis andDesign of Artificial Cognitive Systems*, LNAI 5225, pages 45–62. Springer-Verlag, Berlin Heidelberg.

Calinon, S. and Billard, A. (2009). Statistical learning by imitation of competing constraints in joint space and task space. *Advanced Robotics*, 23(15):2059–2076.

Cangelosi, A. and Riga, T. (2006). An embodied model for sensorimotor grounding and grounding transfer: Experiments with epigenetic robots. *Cognitive Science*, 30(4):673–689.

Clausner, T. (2005). Image schema paradoxes: Implications for cognitive semantics. In Hampe, B., editor, *From Perception to Meaning: Image Schemas in Cognitive Linguistics*, pages 93–110. MOUTON DE GRUYTER, Berlin.

de Saussure, F. (1986). *Course in General Linguistics (Open Court Classics)*. Open Court, Chicago and La Salle, Illinois.

Dominey, P. (2006). From holophrases to abstract grammatical constructions: insights from simulation studies. In Clark, E. and Kelly, B., editors, *Construction in Acquisition*, pages 137–162. CSLI Publications, Stanford CA.

Fodor, J. and Lepore, E. (2002). *The Compositionality Papers*. Oxford University Press, Great Clarendon Street, Oxford.

Gentner, D. and Markman, A. (1997). Structure Mapping in Analogy and Similarity. *American Psychologist*, 52(1):45–56.

Gibson, J. J. (1979). *The Ecological Approach to Visual Perception*. Lawrence Erlbaum Associates, Mahwah, NJ.

Graziano, M. S. A. (2006). The organization of behavioral repertoire in motor cortex. *Annual Review of Neuroscience*, 29:105–134.

Hanson, H. (1959). Effects of discrimination training of stimulus generalization. *Journal of Experimental Psychology*, 7:150–164.

Holmes, N. P. and Spence, C. (2004). The body schema and multisensory representation(s) of peripersonal space. *Cognitive Processing*, 5:94–105.

Johnson, M. (1987). *The Body in the Mind. The Bodily Basis of Meaning*. Chicago University Press, Chicago.

Karmiloff-Smith, A. (1992). *Beyond modularity: A developmental perspective on cognitive science*. MIT Press, Cambridge, MA.

Lakoff, G. (1987). *Women, Fire and Dangerous Things. What Categories reveal about the Mind*. The University of Chicago Press, Chicago.

Mandler, J. (1992). How to build a bady ii: Conceptual primitives. *Psychological Review*, 99(4):587–604.

Markman, A. and Dietrich, E. (1999). Whither structured representation? *Behavioral and Brain Sciences*, 22:626–627. (A commentary on Barsalou (1999)).

Meltzoff, A. (1988a). Imitation, objects, tools, and the rudiments of language in human ontogeny. *Human Evolution*, 3:45–64.

Meltzoff, A. (1988b). Infant imitation and memory: Nine-month-olds in immediate and deferred tests. *Child Development*, 59:217–225.

Nishimoto, R. and Tani, J. (2004). Learning to Generate Combinatorial Action Sequences utilizing the Initial Sensitivity of Deterministic Dynamical Systems. *Neural Networks*, 17(7):925–933.

Pollack, J. (1990). Recursive Distributed Representations. *Artificial Intelligence*, 46:77–105.

Riesenhuber, M. and Poggio, T. (2000). Models of object recognition. *Nature Neuroscience*, 3:1199–1204.

Sugita, Y. and Butz, M. (2010). Towards Emergent Strong Systematicity in a Simple Dynamical Connectionitst Network. Presented at Workshop on Cognitive and neural models for automated processing of speech and text (CONAS2010).

Sugita, Y. and Tani, J. (2005). Learning semantic combinatoriality from the interaction between linguistic and behavioral processes. *Adaptive Behavior*, 13(1):33–52.

Tani, J., Ito, M., and Sugita, Y. (2004). Self-organization of distributedly represented multiple behavior schemata in a mirror system: reviews of robot experiments using RNNPB. *Neural Networks*, 17:1273–1289.

Tuci, E., Ferrauto, T., Massera, G., and Nolfi, S. (2010). Co-development of linguistic and behavioural skills: Compositional semantics and behaviour generalisation. In *Proceedings of the 11th Int. Conf. on Simulation of Adaptive Behavior (SAB2010)*, pages 523–532. Springer-Verlag, Berlin.

Tversky, A. (1984). Features of Similarity. *Psychological Review*, 84:327–352.